Josephson current through a ferromagnetic bilayer: Beyond the quasiclassical approximation

Hao Meng [1,2] Yajie Ren,[1] Javier E. Villegas,[3] and A. I. Buzdin [2,4]

[1]*School of Physics and Telecommunication Engineering, Shaanxi University of Technology, Hanzhong 723001, China*
[2]*University Bordeaux, LOMA UMR-CNRS 5798, F-33405 Talence Cedex, France*
[3]*Unité Mixte de Physique CNRS/Thales, Université Paris-Sud, Université Paris Saclay, 1 Avenue A. Fresnel, 91767 Palaiseau, France*
[4]*Sechenov First Moscow State Medical University, Moscow, 119991, Russia*

Based on the Bogoliubov–de Gennes equations, we provide an exact numerical solution for the critical current of Josephson junctions with a composite ferromagnetic bilayer. We demonstrate that for the antiparallel orientation of the magnetic moments of the bilayer, the presence of a potential barrier at the bilayer interface results in large oscillations of the critical current as a function of ferromagnet thickness and/or exchange field. Because of this, and remarkably, in the range of small exchange field and thicknesses, the magnetism leads to the increase of the critical current. This effect is well pronounced at low temperature but disappears near T_c. If the potential barrier is replaced by a spin-active barrier at the bilayer interface the conventional 0-π transition, similar to the case of an uniform ferromagnetic Josephson junction, is observed. Strikingly, for a parallel orientation of the magnetic moments of the bilayer, the presence of the spin-active barrier restores the anomalous behavior—potential barrier in the antiparallel case. These behaviors result from the resonant tunneling of Cooper pairs across the composite barrier—an effect related to the spin-dependent Fermi vector in the presence of the ferromagnets' exchange field.

I. INTRODUCTION

In recent years the superconductor (S)-ferromagnet (F) systems attracted a lot of attention due to the possibility to fabricate the new devices based on the superconducting spintronics [1–5]. The properties of different S/F systems may be rather well qualitatively understood in the framework of quasiclassical Eilenberger [6] and Usadel [7] approaches. However, the applicability of these methods assumes that the exchange field h in the ferromagnet should be much smaller than the Fermi energy $h \ll E_F$ and the use of the Usadel equations implies even more restrictive conditions $h\tau \ll 1$, where τ is the electrons scattering time. These circumstances lead to the fact that some subtle qualitative effects may be missed by the quasiclassical approach, see, for example, [8–10]. Moreover, a lot of experimental activities with the S/F heterostructures deal with the strong ferromagnets (or even half-metals [11–13]) for which the quasiclassical approximation cannot provide an adequate quantitative description.

The alternative approach for the analysis of proximity effects in strong ferromagnets is the use of the microscopical approach on the basis of the Bogoliubov–de Gennes (BdG) equations [14]. The exact numerical solutions of these equations may provide additional information to the quasiclassical approach and this method was used in [15–24] and references cited therein. Recently the interesting experimental results were obtained for the Josephson junctions containing a ferromagnetic spin valve [25–31]. Taking in mind these experiments in the present work we study the SFS junctions with a composite F layer consisting of two parallel or antiparallel ferromagnetic layers separated by either a potential or a spin-active barrier.

Note that previously the Josephson junctions with ferromagnetic bilayers were studied theoretically by different methods [15–19,32–39] . However, most of the theoretical analysis was made in the framework of the quasiclassical approach, while in the present work we discuss some effects which cannot be found by this approach and has not been discussed before. We have calculated the critical current of the Josephson junctions with a composite (spin-valve) F_1F_2 interlayer and studied the role of the potential and spin-active barrier at the F_1/F_2 interface. The obtained results show an anomalous behavior of the critical current as a function of the exchange field and/or F layer thickness which is very sensitive to the type of barrier at the F_1/F_2 interface.

II. MODEL AND FORMULA

The considered SF_1F_2S Josephson junction with a central potential or spin-active barrier is shown schematically in Fig. 1. The x axis is chosen to be perpendicular to the layer interfaces with the origin located at the central F_1/F_2 interface. The BCS mean-field effective Hamiltonian is [2,14]

$$H_{\text{eff}} = \sum_{\alpha,\beta} \int d\mathbf{r}\{\hat{\psi}_\alpha^\dagger(\mathbf{r})[H_e - (h_z\hat{\sigma}_z)_{\alpha\alpha}]\hat{\psi}_\alpha(\mathbf{r})$$
$$+ \frac{1}{2}[(i\hat{\sigma}_y)_{\alpha\beta}\Delta(\mathbf{r})\hat{\psi}_\alpha^\dagger(\mathbf{r})\hat{\psi}_\beta^\dagger(\mathbf{r}) + \text{H.c.}]$$
$$+ \hat{\psi}_\alpha^\dagger(\mathbf{r})(U\hat{\sigma}_0 - \vec{\rho}\cdot\vec{\sigma})_{\alpha\beta}\hat{\psi}_\beta(\mathbf{r})\}, \quad (1)$$

where $H_e = -\frac{\hbar^2\nabla^2}{2m} - E_F$, and $\hat{\psi}_\alpha^\dagger(\mathbf{r})$ and $\hat{\psi}_\alpha(\mathbf{r})$ represent creation and annihilation operators with spin α. σ_0 denotes a 2×2 unit matrix, and $\vec{\sigma} = (\hat{\sigma}_x, \hat{\sigma}_y, \hat{\sigma}_z)$ is the vector of Pauli
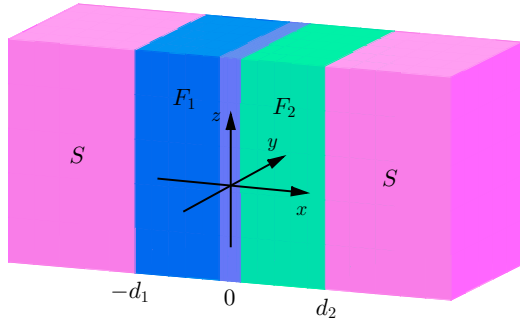
FIG. 1. The sketch of the SF_1F_2S Josephson junction with a potential or spin-active barrier at F_1/F_2 interface. The lengths of F_1 and F_2 are denoted by d_1 and d_2, respectively.

matrices. Here m denotes the effective mass of the quasiparticles in both the superconductors and the ferromagnets and E_F is the Fermi energy. We assume equal Fermi energies in the different regions of the junction. The superconducting gap is supposed to be constant in the superconducting leads and absent inside the ferromagnetic region:

$$\Delta(\mathbf{r}) = \begin{cases} \Delta e^{i\phi/2}, & x < -d_1, \\ 0, & -d_1 < x < d_2, \\ \Delta e^{-i\phi/2}, & x > d_2, \end{cases} \quad (2)$$

where Δ is the magnitude of the gap, and ϕ is the phase difference between the two superconducting leads. This approximation is justified when, for example, the width of the superconducting layers is much larger than the width of F layers. We model the central F_1/F_2 interface by a δ function potential barrier which consists of a spin-independent part $U = V_0\delta(x)$ and a spin-active part $\vec{\rho} = (\rho_x, \rho_y, \rho_z)\delta(x)$. The exchange field in two ferromagnetic layers is parallel or antiparallel to the z axis. It has the form

$$h_z = \begin{cases} h_1\hat{z}, & -d_1 < x < 0, \\ \pm h_2\hat{z}, & 0 < x < d_2, \end{cases} \quad (3)$$

where $\hat{z}$ is the unit vector along the z axis.

To diagonalize the effective Hamiltonian, we use the Bogoliubov transformation $\hat{\psi}_\alpha(\mathbf{r}) = \sum_n [u_{n\alpha}(\mathbf{r})\hat{\gamma}_n + v_{n\alpha}^*(\mathbf{r})\hat{\gamma}_n^\dagger]$ and take into account the anticommutation relations of the quasiparticle annihilation operator $\hat{\gamma}_n$ and creation operator $\hat{\gamma}_n^\dagger$. Using the presentation $u_{n\alpha}(\mathbf{r}) = u_p^\alpha e^{ipx}$, $v_{n\alpha}(\mathbf{r}) = v_p^\alpha e^{ipx}$, the resulting Bogoliubov–de Gennes (BdG) equations can be expressed as [14]

$$\begin{pmatrix} \hat{H}_0 + \hat{V}\delta(x) & i\hat{\sigma}_y\Delta(x) \\ -i\hat{\sigma}_y\Delta^*(x) & -\hat{H}_0 - \hat{V}^*\delta(x) \end{pmatrix} \begin{pmatrix} \hat{u}(x) \\ \hat{v}(x) \end{pmatrix} = \epsilon \begin{pmatrix} \hat{u}(x) \\ \hat{v}(x) \end{pmatrix}, \quad (4)$$

where

$$\hat{H}_0 = \begin{pmatrix} \xi_p - h_z & 0 \\ 0 & \xi_p + h_z \end{pmatrix}$$

and

$$\hat{V} = \begin{pmatrix} V_0 - \rho_z & -(\rho_x - i\rho_y) \\ -(\rho_x + i\rho_y) & V_0 + \rho_z \end{pmatrix}.$$

Here $\xi_p = \frac{\hbar^2 p^2}{2m} - E_F$, and $\hat{u}(x) = [u_p^\uparrow(x), u_p^\downarrow(x)]^T$ and $\hat{v}(x) = [v_p^\uparrow(x), v_p^\downarrow(x)]^T$ are quasiparticle and quasihole wave functions, respectively.

The BdG equation (4) can be solved for each superconducting electrode and each ferromagnetic layer, respectively. For a given energy ϵ in the superconducting gap, we find the following plane-wave solutions in the left superconducting electrode:

$$\psi_L^S(x) = C_1\hat{\zeta}_1 e^{-ik_S^+ x} + C_2\hat{\zeta}_2 e^{ik_S^- x}$$
$$+ C_3\hat{\zeta}_3 e^{-ik_S^+ x} + C_2\hat{\zeta}_4 e^{ik_S^- x}, \quad (5)$$

where $k_S^\pm = k_F\sqrt{1 \pm i\sqrt{\Delta^2 - \epsilon^2}/E_F - (k_\parallel/k_F)^2}$ are the longitudinal components of the wave vectors for quasiparticles in both superconductors. $\hat{\zeta}_1 = [1, 0, 0, R_1 e^{-i\phi/2}]^T$, $\hat{\zeta}_2 = [1, 0, 0, R_2 e^{-i\phi/2}]^T$, $\hat{\zeta}_3 = [0, 1, -R_1 e^{-i\phi/2}, 0]^T$, and $\hat{\zeta}_4 = [0, 1, -R_2 e^{-i\phi/2}, 0]^T$ are the four basis wave functions of the left superconductor, in which $R_{1(2)} = (\epsilon \mp i\sqrt{\Delta^2 - \epsilon^2})/\Delta$. The corresponding wave function in the right superconducting electrode can be described by

$$\psi_R^S(x) = D_1\hat{\eta}_1 e^{ik_S^+ x} + D_2\hat{\eta}_2 e^{-ik_S^- x}$$
$$+ D_3\hat{\eta}_3 e^{ik_S^+ x} + D_4\hat{\eta}_4 e^{-ik_S^- x}, \quad (6)$$

where $\hat{\eta}_1 = [1, 0, 0, R_1 e^{i\phi/2}]^T$, $\hat{\eta}_2 = [1, 0, 0, R_2 e^{i\phi/2}]^T$, $\hat{\eta}_3 = [0, 1, -R_1 e^{i\phi/2}, 0]^T$, and $\hat{\eta}_4 = [0, 1, -R_2 e^{i\phi/2}, 0]^T$.

The wave function in the F_1 layer is

$$\psi_{F_1}(x) = (M_1 e^{ik_1 x} + M_1' e^{-ik_1 x})\hat{e}_1 + (M_2 e^{ik_2 x} + M_2' e^{-ik_2 x})\hat{e}_2$$
$$+ (M_3 e^{ik_3 x} + M_3' e^{-ik_3 x})\hat{e}_3 + (M_4 e^{ik_4 x} + M_4' e^{-ik_4 x})\hat{e}_4, \quad (7)$$

where $\hat{e}_1 = (1\,0\,0\,0)^T$, $\hat{e}_2 = (0\,1\,0\,0)^T$, $\hat{e}_3 = (0\,0\,1\,0)^T$, and $\hat{e}_4 = (0\,0\,0\,1)^T$ are basis wave functions in the ferromagnetic region, and $k_{1(2)} = k_F\sqrt{1 + (\epsilon \pm h_1)/E_F - (k_\parallel/k_F)^2}$ and $k_{3(4)} = k_F\sqrt{1 - (\epsilon \mp h_1)/E_F - (k_\parallel/k_F)^2}$ are the longitudinal components of the wave vectors for the quasiparticles in the F_1 layer. The corresponding wave function $\psi_{F_2}(x)$ in the F_2 layer can be obtained from Eq. (7) by replacement $h_1 \rightarrow h_2$. It is worthy to note that the parallel component $k_\parallel$ is conserved in transport processes of the quasiparticles.

The wave functions $[\psi_L^S(x), \psi_{F1}(x), \psi_{F2}(x),$ and $\psi_R^S(x)]$ and their first derivatives should satisfy the boundary conditions at the S/F_1, F_1/F_2, and F_2/S interfaces,

$$\psi_L^S(-d_1) = \psi_{F1}(-d_1),$$

$$\frac{\partial\psi_L^S}{\partial x}\bigg|_{x=-d_1} = \frac{\partial\psi_{F1}}{\partial x}\bigg|_{x=-d_1}, \quad (8)$$

$$\psi_{F1}(0) = \psi_{F2}(0),$$

$$\frac{d\psi_{F2}}{dx}\bigg|_{x=0^+} - \frac{d\psi_{F1}}{dx}\bigg|_{x=0^-} = k_F \begin{pmatrix} \hat{W} & 0 \\ 0 & \hat{W}^* \end{pmatrix}\psi(0), \quad (9)$$

$$\psi_{F2}(d_2) = \psi_R^S(d_2),$$

$$\frac{\partial\psi_{F2}}{\partial x}\bigg|_{x=d_2} = \frac{\partial\psi_R^S}{\partial x}\bigg|_{x=d_2}, \quad (10)$$

where

$$\hat{W} = \begin{pmatrix} Z - P_z & -(P_x - iP_y) \\ -(P_x + iP_y) & Z + P_z \end{pmatrix}. \quad (11)$$

We define the dimensionless spin-independent parameter $Z = 2mV_0/(\hbar^2 k_F)$ measuring the strength of the potential

barrier and the dimensionless spin-dependent parameter $P_{x,y,z} = 2m\rho_{x,y,z}/(\hbar^2 k_F)$ describing the spin-active barrier at the F_1/F_2 interface. For simplicity we just consider the effect of y-component P_y and ignore the role of x and z components (P_x and P_z).

From these boundary conditions we can set up 24 linear equations in the following form:

$$\hat{A}X = \hat{B},\tag{12}$$

where X contains 24 scattering coefficients and $\hat{A}$ is a 24×24 matrix. The solution of the characteristic equation

$$\det \hat{A} = 0\tag{13}$$

allows one to identify two Andreev bound-state solutions for energies $E_{A\omega}$ ($\omega = 1, 2$). Below we will consider the case of the short Josephson junction with a thickness much smaller than the superconducting coherence length ξ. In such a case the main contribution to the Josephson current is provided by the Andreev bound states (see, e.g., [40,41]). In a one-dimensional (1D) SF_1F_2S junction, the Josephson current can be calculated by the general formula

$$I^{1D}(\phi) = \frac{2e}{\hbar}\frac{\partial\Omega}{\partial\phi},\tag{14}$$

where Ω is the phase-dependent thermodynamic potential. This potential can be obtained from the excitation spectrum by using the formula [42,43]

$$\Omega = -2T\sum_\omega \ln\left[2\cosh\frac{E_{A\omega}(\phi)}{2T}\right],\tag{15}$$

where Δ, h_1, h_2, Z, and P_y are assumed to be the equilibrium values, which minimize the free energy of the SF_1F_2S structure and depend on microscopic parameters [44]. The summation in (15) is taken over all positive Andreev energies $[0 < E_{A\omega}(\phi) < \Delta]$. For each value of ϕ, we solve Eq. (13) numerically to obtain the two spin-polarized Andreev levels. Since the Andreev energy spectra are doubled as they include the Bogoliubov redundancy, and only half of the energy states should be taken into account, we can find the 1D Josephson current via Eqs. (14) and (15).

In a three-dimensional (3D) case, the Josephson current can be expressed as

$$\begin{aligned}I^{3D}(\phi) &= \frac{S}{4\pi^2}\frac{2e\Delta}{\hbar}\int_0^{k_F} I^{1D}(k_\parallel)2\pi k_\parallel dk_\parallel\\ &= \frac{4\pi\Delta}{eR_N}\int_0^1 I^{1D}(\tilde{k}_\parallel)\tilde{k}_\parallel d\tilde{k}_\parallel,\end{aligned}\tag{16}$$

where $R_N^{-1} = e^2 k_F^2 S/(4\pi^2\hbar)$ is the Sharvin resistance and $\tilde{k}_\parallel = k_\parallel/k_F$ is the normalized wave vector. The 3D critical current can be derived from $I_c^{3D} = \max_\phi |I^{3D}(\phi)|$.

III. RESULTS AND DISCUSSIONS

In our calculations we use the superconducting gap Δ as a unit of energy and take the Fermi energy $E_F = 1000\Delta$. All lengths and the exchange field strengths are measured in units of the inverse Fermi wave vector k_F and the Fermi energy E_F, respectively. Note that the approximation of the short
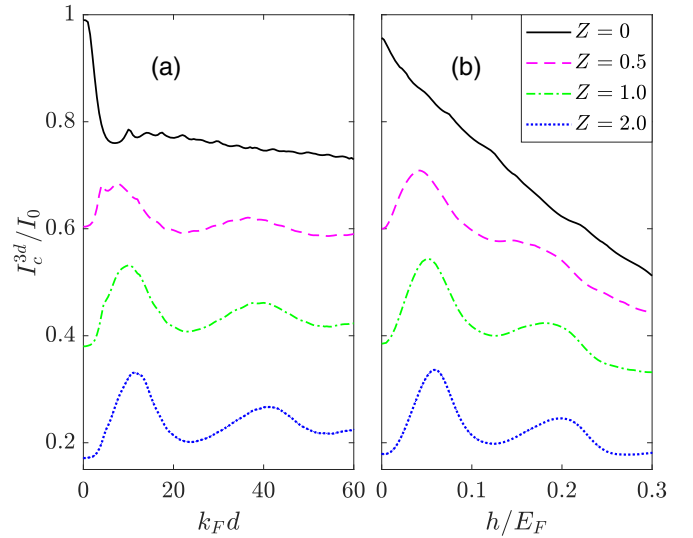

FIG. 2. The dependence of the 3D critical current I_c^{3D} on the ferromagnetic thickness $k_F d$ for the exchange field $h/E_F = 0.1$ (a) and on the exchange field h/E_F for the ferromagnetic thickness $k_F d = 20$ (b) when the potential barrier Z takes several different values. Here we consider an antiparallel orientation of the exchange fields.

Josephson junction ($k_F d_1$, $k_F d_2 \ll 1000$) is fully satisfied in the presented calculations. The normalized unit of current is $I_0 = 2\pi\Delta/(eR_N)$ in the 3D case.

We study the SF_1F_2S structures with a potential barrier Z or a spin-active barrier P_y at the F_1/F_2 interface. We present the results for $h_1 = h_2 = h$ for parallel exchange field and $h_1 = -h_2 = h$ for antiparallel exchange field, and define the ferromagnetic thickness $d_1 = d_2 = d$.

We draw in Fig. 2 the dependence of the critical current I_c^{3D} on the ferromagnetic thickness $k_F d$ and the exchange field h/E_F for an antiparallel alignment of the magnetic moment $h_1 = -h_2 = h$ when the potential barrier Z takes several different values. It is shown that the critical current decreases monotonically with the increasing exchange field for the transparent F_1/F_2 interface $Z = 0$, while it reveals the oscillating behavior for $Z > 0$. By increasing Z, the amplitude of the critical current decreases as a whole, but the oscillation behavior still remains. The critical current shows the same characteristic if one increases the ferromagnetic thickness $k_F d$. These features indicate that the oscillation of the critical current originates from the resonant tunneling of the Cooper pairs occurring between the F_1 and F_2 layers. In fact the spin-dependent wave vector of the pairing electrons will change when the Cooper pairs pass through the F_1 and F_2 layer, and therefore the phase evolution of the Cooper pairs leads to the resonances occurring in F_1 and F_2. Therefore, the oscillation period depends on the exchange field and/or thickness of the ferromagnets, not on the properties of the central insulating barrier.

If one changes the exchange field h/E_F and thickness $k_F d$ of the ferromagnetic layers, the oscillation period of the critical current changes accordingly. The calculation results are illustrated in Fig. 3. The observed oscillations remind us of the oscillations observed previously in [19] for the 1D model
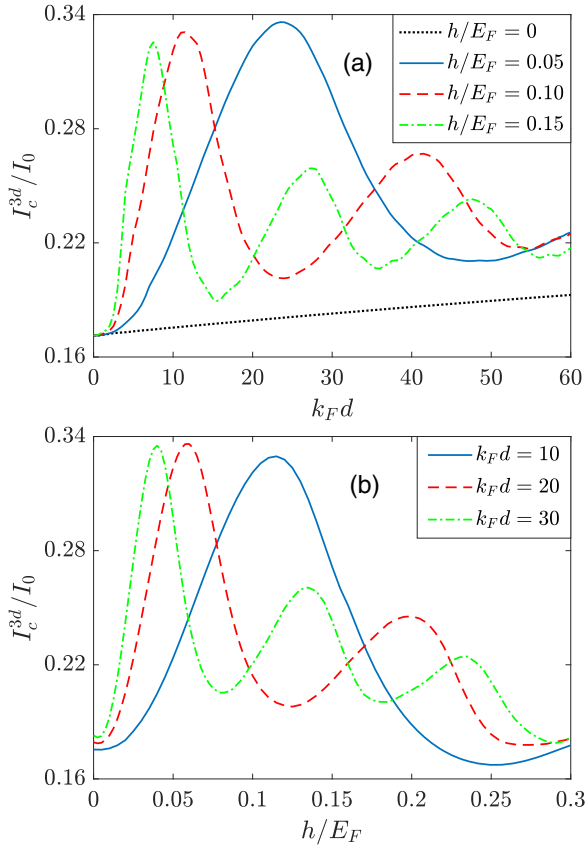
FIG. 3. The dependence of the 3D critical current I_c^{3D} on the ferromagnetic thickness $k_F d$ (a) and on the exchange field h/E_F (b) in the case of an antiparallel orientation. Here the potential barrier is $Z = 2$.

of the junction with noncollinear magnetization and attributed to the geometrical resonances. The interesting consequence of the presence of barrier is the counterintuitive increase of the critical current with increasing exchange field [up to $h_{max}/E_F \sim 0.12$ when $k_F d = 10$, see Fig. 3(b)] or ferromagnetic layer thickness [up to $k_F d_{max} \sim 24$ when $h/E_F = 0.05$, see Fig. 3(a)]. Note that the similar increase of the current with the exchange field was obtained in the models of S/F tunnel structures [34–36]. The key difference between our results and Refs. [34–36] is that the initial increase was not followed by the oscillatory behavior of the critical current with exchange field and/or ferromagnetic layer thickness. We find also that the growth range of the critical current with the exchange field strongly depends on the ferromagnetic layer thicknesses. Moreover, note that in presence of a potential barrier the critical current slightly increases with normal-metal thickness when both ferromagnets become the normal-metal ($h/E_F = 0$) [see Fig. 3(a)]. This circumstance reflects the presence of some resonance effects in this case too. It should be noted that the oscillatory effect mentioned above is revealed only at low temperatures. The dependence of the critical current on the temperature is illustrated in Fig. 4. We see that the oscillations of the critical current I_c^{3D} will decrease as the temperature T/Δ increases, which should be related to the smearing of the resonance tunneling from the lowest Andreev levels. When T/Δ reaches 0.9, the oscillation completely disappears and I_c^{3d} decreases monotonously.
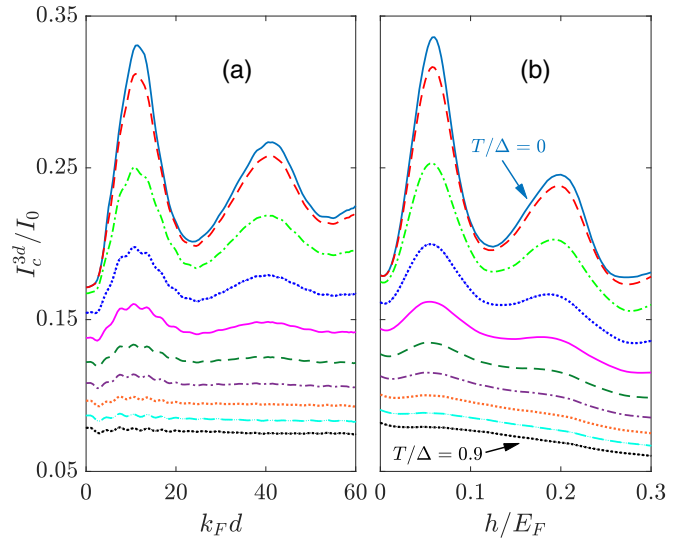

FIG. 4. The dependence of the 3D critical current I_c^{3D} on the ferromagnetic thickness $k_F d$ for the exchange field $h/E_F = 0.1$ (a) and on the exchange field h/E_F for the ferromagnetic thickness $k_F d = 20$ (b) in the case of an antiparallel orientation. Here the temperature T/Δ varies from 0 to 0.9 with a step 0.1, which corresponds to the curves from top to bottom. The potential barrier is $Z = 2$.
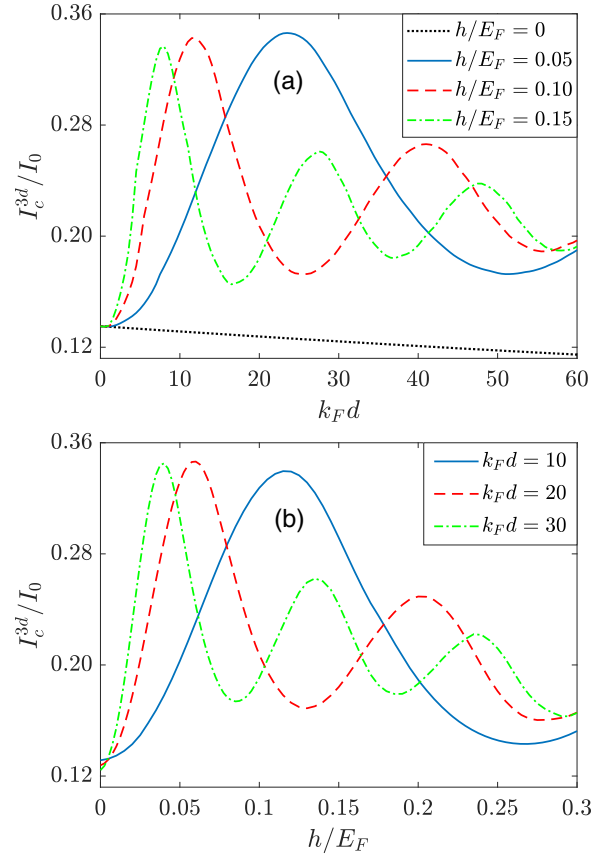

FIG. 5. The dependence of the 3D critical current I_c^{3D} on the ferromagnetic thickness $k_F d$ (a) and on the exchange field h/E_F (b) in the case of a parallel orientation. Here the spin-active barrier is taken as $P_y = 2$.
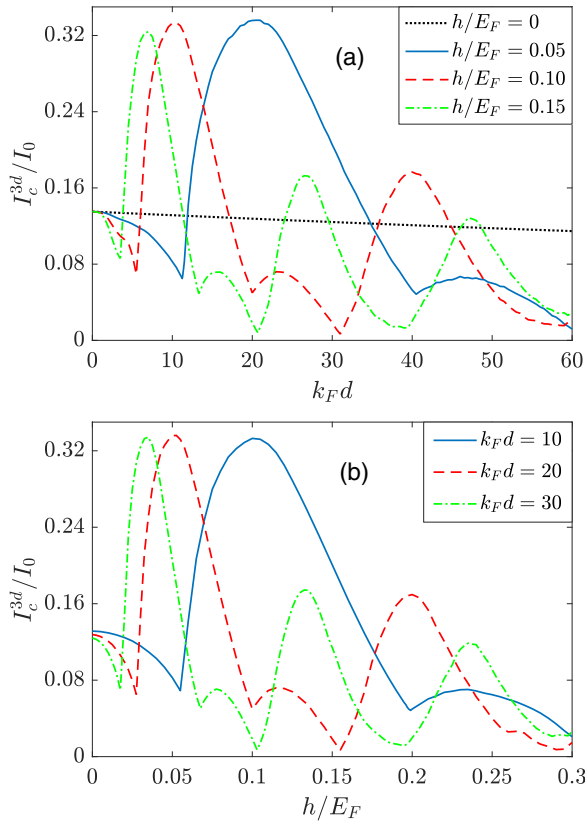
FIG. 6. The dependence of the 3D critical current I_c^{3D} on the ferromagnetic thickness $k_F d$ (a) and on the exchange field h/E_F (b) in the case of an antiparallel orientation. Here the spin-active barrier is taken as $P_y = 2$. The dips at the curves signal the transitions between 0 and π states.
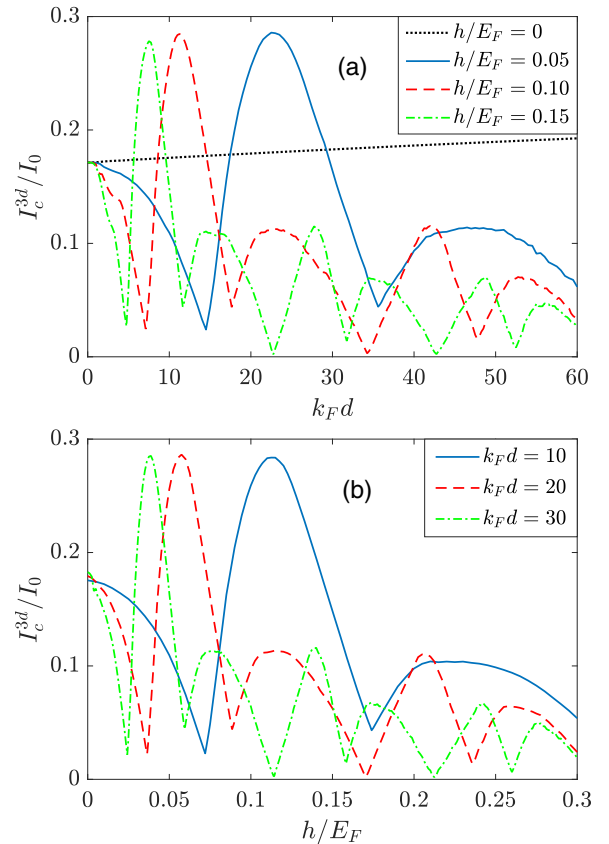

FIG. 7. The dependence of the 3D critical current I_c^{3D} on the ferromagnetic thickness $k_F d$ (a) and on the exchange field h/E_F (b) in the case of a parallel orientation. Here the potential barrier is taken as $Z = 2$. The dips at the curves signal the transitions between 0 and π states.

In Fig. 5 we show the variation characteristics of the critical current in SF_1F_2S structure with the magnetic moment in F_1 and F_2 being parallel and with a spin-active barrier at the F_1/F_2 interface. It is found that the critical current also displays an oscillating behavior. The behavior is similar to the cases in which the magnetic moments are antiparallel and there is a potential barrier at the F_1/F_2 interface. So we can say that the spin-active barrier at the F_1/F_2 interface can play two roles: (i) It creates a spin-flip effect to flip the spin of the conduction electrons crossing the F_1/F_2 interface. The two ferromagnets have the same energy band because of the parallel polarized direction of the magnetic moments. In such a case, spin-↑ (↓) electrons will be transformed into spin-↓ (↑) electrons when they pass from the F_1 layer into the F_2 layer. The same electron will occupy the opposite spin band in the F_1 and F_2 layers. This situation is similar to the antiparallel ferromagnets without the spin-flip in the central interface. (ii) It acts as a potential barrier, which hinders electron tunneling and reduces the transmission of the F_1/F_2 interface. Therefore, we can still see the oscillating phenomenon of the critical current in this structure.

Similarly, the above two roles caused by the spin-active barrier can also present in the antiparallel SF_1F_2S junction. If one only considers the role of the spin-flip effect, the antiparallel SF_1F_2S junction with a central spin-flip is equivalent to a homogeneous SFS junction. In this case, the 0-π transition

will resume. For example, at $h/E_F = 0.05$ the inversion of the current sign takes place at $k_F d \approx 10$ and $k_F d \approx 40$ (see Fig. 6(a) and Fig. 1 in the Supplemental Material [45]). In other words, the junction is in π state for $k_F d \prec 10$ and $k_F d \succ 40$, as well as it will become 0 state in the region $10 \prec k_F d \prec 40$. Moreover, the insulating property of the spin-active barrier causes a resonant tunneling of electrons. This results in the largest peaks that appear periodically in the current I_c^{3D}. For example, if one looks at the curve for $h/E_F = 0.10$ in Fig 6(a), the resonance produces the peaks at $k_F d \approx 10$ and $k_F d \approx 40$, which appear in similar positions in Fig. 3(a).

To further demonstrate the coexistence of resonant tunneling and 0-π transition, we calculated the current in the parallel SF_1F_2S junction with a central potential barrier. It is known that, in a uniform SFS junction, the critical current decays with increasing ferromagnetic thickness (or exchange field) and also reveals oscillations caused by the 0-π transition. If the potential barrier is introduced at the center of the ferromagnet, the amplitude of the critical current will be suppressed overall because the potential barrier reduces the transmission of the conduction electrons. Meanwhile, the resonant tunneling of the conduction electrons between F_1 and F_2 layers induces the periodic peaks in the critical current. As a result, the critical current shows singular features in Fig. 7 and Fig. 2 of the Supplemental Material [45].
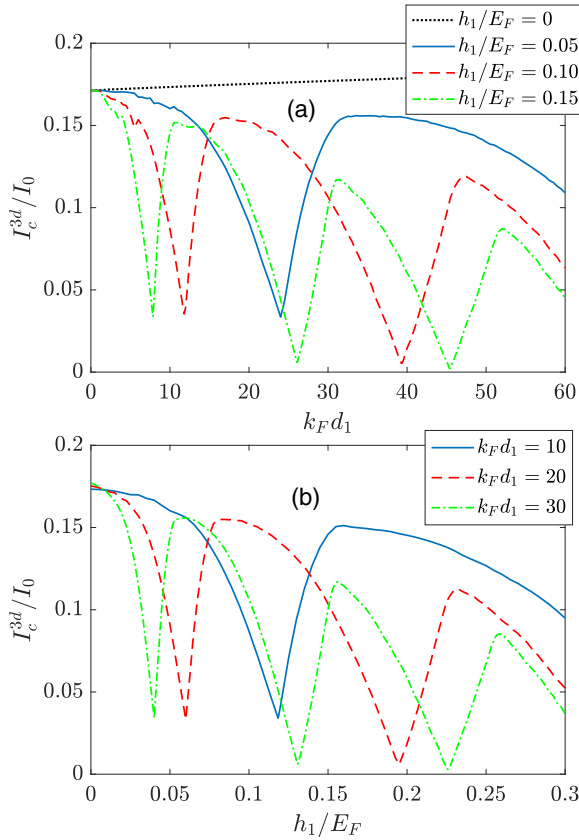
FIG. 8. The dependence of the 3D critical current I_c^{3D} on the ferromagnetic thickness $k_F d_1$ (a) and on the exchange field h_1/E_F (b) for the SF_1S configuration ($d_2 = 0$) with the potential barrier $Z = 2$ at the right F_1/S interface. The dips at the curves signal the transitions between 0 and π states.
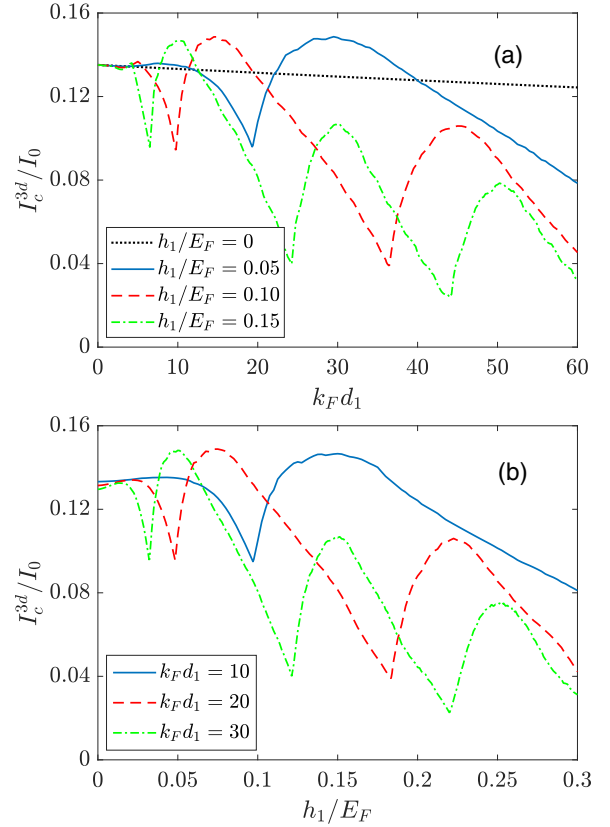

FIG. 9. The dependence of the 3D critical current I_c^{3D} on the ferromagnetic thickness $k_F d_1$ (a) and on the exchange field h_1/E_F (b) for the SF_1S configuration ($d_2 = 0$) with the spin-active barrier $P_y = 2$ at the right F_1/S interface. The dips at the curves signal the transitions between 0 and π states.

Finally, in order to illustrate the previous conjecture regarding resonant tunneling, we discuss the current in the SF_1S junction ($d_2 = 0$) with the potential or spin-active barriers at the F_1/S interface. As shown in Figs. 8 and 9, the critical current displays a damped oscillation with increasing thickness $k_F d_1$ and/or exchange field h_1/E_F. These current oscillations can be attributed to the 0-π transition (see Figs. 3 and 4 in the Supplemental Material [45]) but not to the periodic peaks induced by the resonant tunneling between the F_1 and F_2 layers, because the resonant tunneling cannot exist in these structures. In addition, we find that the critical current at the transition between the 0 and π states is close to zero in the SF_1S junction with the potential barrier $Z = 2$ at the F_1/S interface, when the thickness $k_F d_1$ and/or exchange field h_1/E_F take larger values. However, this current is much larger when the F_1/S interface has a spin-active barrier $P_y = 2$ (see Fig. 9). This may be related to the important contribution from the second harmonic current in the presence of spin-active interface structure [34,46–48].

IV. CONCLUSION

On the basis of the exact numerical solution of the Bogoliubov–de Gennes equations, we have studied the Josephson current in the SF_1F_2S junctions containing a potential or spin-active barrier at the F_1/F_2 interface. We show

that at low temperature the potential barrier may result in large oscillations of the critical current as a function of the ferromagnetic layer thickness and exchange field even for the antiparallel orientation of the magnetic moment in the F_1 and F_2 layers. Such behavior is related to the interference effects of the electrons wave functions and may be considered as some form of the geometrical resonance phenomena. Specifically, comparing to the normal-metal junction ($h = 0$ in our model), the exchange field ($h > 0$) can enhance the critical current for the antiparallel configuration. In contrast, the spin-active barrier in this antiparallel configuration leads to the 0-π transitions, which is similar to the case of the uniform SFS junction. The spin-active barrier in the parallel configuration can also cause the oscillations of the critical current. The obtained results may be useful for the interpretation of the experimental data on the Josephson junctions with a composite ferromagnetic barrier.

[1] A. A. Golubov, M. Yu. Kupriyanov, and E. Ilichev, The current-phase relation in Josephson junctions, Rev. Mod. Phys. **76**, 411 (2004).

[2] A. I. Buzdin, Proximity effects in superconductor-ferromagnet heterostructures, Rev. Mod. Phys. **77**, 935 (2005).

[3] F. S. Bergeret, A. F. Volkov, and K. B. Efetov, Odd triplet superconductivity and related phenomena in superconductor-ferromagnet structures, Rev. Mod. Phys. **77**, 1321 (2005).

[4] J. Linder and J. W. A. Robinson, Superconducting spintronics, Nat. Phys. **11**, 307 (2015).

[5] M. Eschrig, Spin-polarized supercurrents for spintronics: A review of current progress, Rep. Prog. Phys. **78**, 104501 (2015).

[6] G. Eilenberger, Transformation of Gorkov's equation for type II superconductors into transport-like equations, Z. Phys. **214**, 195 (1968).

[7] K. D. Usadel, Generalized Diffusion Equation for Superconducting Alloys, Phys. Rev. Lett. **25**, 507 (1970).

[8] C. R. Reeg and D. L. Maslov, Proximity-induced triplet superconductivity in Rashba materials, Phys. Rev. B **92**, 134512 (2015).

[9] M. A. Silaev, I. V. Tokatly, and F. S. Bergeret, Anomalous current in diffusive ferromagnetic Josephson junctions, Phys. Rev. B **95**, 184508 (2017).

[10] H. Meng, A. V. Samokhvalov, and A. I. Buzdin, Nonuniform superconductivity and Josephson effect in a conical ferromagnet, Phys. Rev. B **99**, 024503 (2019).

[11] C. Visani, Z. Sefrioui, J. Tornos, C. Leon, J. Briatico, M. Bibes, A. Barthélémy, J. Santamaría, and J. E. Villegas, Equal-spin Andreev reflection and long-range coherent transport in high-temperature superconductor/half-metallic ferromagnet junctions, Nat. Phys. **8**, 539 (2012).

[12] C. Visani, F. Cuellar, A. Pérez-Muñoz, Z. Sefrioui, C. León, J. Santamaría, and J. E. Villegas, Magnetic field influence on the proximity effect at YBa$_2$Cu$_3$O$_7$/La$_{2/3}$Ca$_{1/3}$MnO$_3$ superconductor/half-metal interfaces, Phys. Rev. B **92**, 014519 (2015).

[13] M. Egilmez, J. W. A. Robinson, J. L. MacManus-Driscoll, L. Chen, H. Wang, and M. G. Blamire, Supercurrents in half-metallic ferromagnetic La$_{0.7}$Ca$_{0.3}$MnO$_3$, Europhys. Lett. **106**, 37003 (2014).

[14] P. G. de Gennes, *Superconductivity of Metals and Alloys* (Benjamin, New York, 1966), Chap. 5.

[15] Z. Radović, N. Lazarides, and N. Flytzanis, Josephson effect in double-barrier superconductor-ferromagnet junctions, Phys. Rev. B **68**, 014501 (2003).

[16] K. Halterman and O. T. Valls, Layered ferromagnet-superconductor structures: The π state and proximity effects, Phys. Rev. B **69**, 014517 (2004).

[17] P. H. Barsic, O. T. Valls, and K. Halterman, Thermodynamics and phase diagrams of layered superconductor/ferromagnet nanostructures, Phys. Rev. B **75**, 104502 (2007).

[18] K. Halterman, O. T. Valls, and C.-T. Wu, Charge and spin currents in ferromagnetic Josephson junctions, Phys. Rev. B **92**, 174516 (2015).

[19] Z. Pajović, M. Božović, Z. Radović, J. Cayssol, and A. Buzdin, Josephson coupling through ferromagnetic heterojunctions with noncollinear magnetizations, Phys. Rev. B **74**, 184509 (2006).

[20] K. Halterman and M. Alidoust, Half-metallic superconducting triplet spin valve, Phys. Rev. B **94**, 064503 (2016).

[21] K. Halterman and M. Alidoust, Josephson currents and spin-transfer torques in ballistic SFSFS nanojunctions, Supercond. Sci. Technol. **29**, 055007 (2016).

[22] M. Alidoust and K. Halterman, Half-metallic superconducting triplet spin multivalves, Phys. Rev. B **97**, 064517 (2018).

[23] K. Halterman and M. Alidoust, Induced energy gap in finite-sized superconductor/ferromagnet hybrids, Phys. Rev. B **98**, 134510 (2018).

[24] C.-T. Wu and K. Halterman, Spin transport in half-metallic ferromagnet-superconductor junctions, Phys. Rev. B **98**, 054518 (2018).

[25] C. Bell, G. Burnell, C. W. Leung, E. J. Tarte, D.-J. Kang, and M. G. Blamire, Controllable Josephson current through a pseudospin-valve structure, Appl. Phys. Lett. **84**, 1153 (2004).

[26] J. W. A. Robinson, G. B. Halasz, A. I. Buzdin, and M. G. Blamire, Enhanced Supercurrents in Josephson Junctions Containing Nonparallel Ferromagnetic Domains, Phys. Rev. Lett. **104**, 207001 (2010).

[27] B. Baek, W. H. Rippard, S. P. Benz, S. E. Russek, and P. D. Dresselhaus, Hybrid superconducting-magnetic memory device using competing order parameters, Nat. Commun. **5**, 3888 (2014).

[28] M. A. E. Qader, R. K. Singh, S. N. Galvi, L. Yu, J. M. Rowell, and N. Newman, Switching at small magnetic fields in Josephson junctions fabricated with ferromagnetic barrier layers, Appl. Phys. Lett. **104**, 022602 (2014).

[29] B. Baek, W. H. Rippard, M. R. Pufall, S. P. Benz, S. E. Russek, H. Rogalla, and P. D. Dresselhaus, Spin-Transfer Torque Switching in Nanopillar Superconducting-Magnetic Hybrid Josephson Junctions, Phys. Rev. Appl. **3**, 011001 (2015).

[30] E. C. Gingrich, B. M. Niedzielski, J. A. Glick, Y. Wang, D. L. Miller, R. Loloee, W. P. Pratt, Jr., and N. O. Birge, Controllable 0-π Josephson junctions containing a ferromagnetic spin valve, Nat. Phys. **12**, 564 (2016).

[31] B. M. Niedzielski, T. J. Bertus, J. A. Glick, R. Loloee, W. P. PrattJr., and N. O. Birge, Spin-valve Josephson junctions for cryogenic memory, Phys. Rev. B **97**, 024517 (2018).

[32] A. V. Samokhvalov, R. I. Shekhter, and A. I. Buzdin, Stimulation of a singlet superconductivity in SFS weak links by spin-exchange scattering of Cooper pairs, Sci. Rep. **4**, 5671 (2014).

[33] I. Kulagina and J. Linder, Spin supercurrent, magnetization dynamics, and φ-state in spin-textured Josephson junctions, Phys. Rev. B **90**, 054504 (2014).

[34] F. S. Bergeret, A. F. Volkov, and K. B. Efetov, Enhancement of the Josephson Current by an Exchange Field in Superconductor-Ferromagnet Structures, Phys. Rev. Lett. **86**, 3140 (2001).

[35] V. N. Krivoruchko and E. A. Koshina, From inversion to enhancement of the dc Josephson current in S/F-I-F/S tunnel structures, Phys. Rev. B **64**, 172511 (2001).

[36] E. Koshina and V. Krivoruchko, Spin polarization and π-phase state of the Josephson contact: Critical current of mesoscopic SFIFS and SFIS junctions, Phys. Rev. B **63**, 224515 (2001).

[37] A. A. Golubov, M. Yu. Kupriyanov, and Ya. V. Fominov, Critical current in SFIFS junctions, Pis'ma Zh. Eksp. Teor. Fiz. **75**, 223 (2002) [JETP Lett. **75**, 190 (2002)].

[38] Ya. M. Blanter and F. W. J. Hekking, Supercurrent in long SFFS junctions with antiparallel domain configuration, Phys. Rev. B **69**, 024525 (2004).

[39] B. Crouzy, S. Tollis, and D. A. Ivanov, Josephson current in a superconductor-ferromagnet junction with two noncollinear magnetic domains, Phys. Rev. B **75**, 054503 (2007).

[40] P. F. Bagwell, Suppression of the Josephson current through a narrow, mesoscopic, semiconductor channel by a single impurity, Phys. Rev. B **46**, 12573 (1992).

[41] C. W. J. Beenakker, Universal Limit of Critical-Current Fluctuations in Mesoscopic Josephson Junctions, Phys. Rev. Lett. **67**, 3836 (1991).

[42] J. Bardeen, R. Kümel, A. E. Jacobs, and L. Tewordt, Structure of vortex lines in pure superconductors, Phys. Rev. **187**, 556 (1969).

[43] J. Cayssol and G. Montambaux, Exchange-induced ordinary reflection in a single-channel superconductor-ferromagnet-superconductor junction, Phys. Rev. B **70**, 224520 (2004).

[44] L. N. Bulaevskii, A. I. Buzdin, M. L. Kulić, and S. V. Panyukov, Coexistence of superconductivity and magnetism theoretical predictions and experimental results, Adv. Phys. **34**, 175 (1985).

[45] See Supplemental Material at http://link.aps.org/supplemental/10.1103/PhysRevB.100.224514 for comparison between the absolute value of critical current $|I_c^{3D}|$ and the original critical current I_c^{3D}.

[46] L. Trifunovic, Long-Range Superharmonic Josephson Current, Phys. Rev. Lett. **107**, 047001 (2011).

[47] C. Richard, M. Houzet, and J. S. Meyer, Superharmonic Long-Range Triplet Current in a Diffusive Josephson Junction, Phys. Rev. Lett. **110**, 217004 (2013).

[48] A. S. Mel'nikov, A. V. Samokhvalov, S. M. Kuznetsova, and A. I. Buzdin, Interference Phenomena and Long-Range Proximity Effect in Clean Superconductor-Ferromagnet Systems, Phys. Rev. Lett. **109**, 237006 (2012).